Deep Space Observations of Sun Glints from Marine Ice Clouds

Tamás Várnai, Alexander B. Kostinski, and Alexander Marshak

***Abstract*— The Earth Polychromatic Camera (EPIC) onboard the Deep Space Climate Observatory (DSCOVR) spacecraft takes images of the sunlit face of the earth from a million miles away. Earlier work showed that EPIC detected the specular reflection of sunlight (i.e., sun glint) from ice crystals floating in cold clouds over land; here we show that this phenomenon can also be detected over oceans. Furthermore, the results show that—using its observations at oxygen A-band absorption bands—EPIC can distinguish glints off marine ice clouds from those off the ocean surface. The analysis of more than two years of EPIC data reveals that the two kinds of glints are detected with comparable frequency. Glints off clouds are shown to be generally brighter but smaller in spatial extent. It is also demonstrated that glints off ice clouds have a discernible effect on the regional mean reflectance and that EPIC observations can help constrain the radiative contribution of oriented ice crystals.**

***Index Terms*— Atmosphere, sensing platforms.**

I. Introduction

THE Earth Polychromatic Camera (EPIC) onboard the Deep Space Climate Observatory (DSCOVR) takes roughly hourly images of the sunlit face of the earth from the Lagrangian L1 point at about a million miles away [1]. The earliest observations by EPIC immediately revealed conspicuous and surprising colored bright spots, which sometimes saturated the detector (see [1]). These bright spots were termed glints because it was shown [2] that specular reflection off ice-containing clouds floating over land was the physical origin of the phenomenon. Here, we pose the question of whether the approach we used in [2] can also detect and characterize glints off marine clouds. To address this question, one must be able to identify the origin of such glints: is it clouds or the underlying ocean surface that is responsible for the specular reflection observed from a million miles away? It turns out that EPIC observations are well suited for this purpose because EPIC's molecular oxygen absorption channels constrain the altitude of the signal's origin.

Manuscript received April 4, 2019; revised June 2, 2019; accepted June 28, 2019. The work of T. Várnai and A. Marshak was supported by the NASA DSCOVR Project. The work of A. B. Kostinski was supported by NSF under Grant AGS-1639868. *(Corresponding author: Tamás Várnai.)*

T. Várnai is with the Joint Center for Earth Systems Technology, University of Maryland, Baltimore, MD 21228 USA, and also with the NASA Goddard Space Flight Center, Greenbelt, MD 20771 USA (e-mail: tamas.varnai@nasa.gov).

A. B. Kostinski is with the Department of Physics, Michigan Technological University, Houghton, MI 49931 USA (e-mail: kostinsk@mtu.edu).

A. Marshak is with the NASA Goddard Space Flight Center, Greenbelt, MD 20771 USA (e-mail: alexander.marshak@nasa.gov).

Color versions of one or more of the figures in this letter are available online at http://ieeexplore.ieee.org.

Digital Object Identifier 10.1109/LGRS.2019.2930866

While path-integrated oxygen absorption was already used in [2] to pinpoint ice clouds as the sources of glint over land, here we demonstrate that one can distinguish marine cloud glints from ocean surface glints. Furthermore, we show that cloud glints are, on average, brighter and more focused than their ocean counterparts; a finding of importance beyond atmospheric science, as astronomers are looking for ocean glints off exoplanets [3], [4]. Finally, we demonstrate the discernible effect of cloud glints on regional mean reflectance and discuss the associated radiative transfer implications for earth's climate. A potential interpretation of glints in terms of cold cloud microphysics is also discussed.

II. Data Analysis and Ocean/Cloud Separation Results

Insofar as the central notion in this work is a specular reflection (glint), we note from the outset a certain observational "fuzziness" in the assignment of specular direction caused by the finite angular size of the sun, 0.5°, present even for a perfectly smooth earth surface. Furthermore, EPIC's spatial resolution is about 10 km, and thus, the normal direction to the earth surface changes by roughly 0.1° within a pixel. Since the EPIC view direction is the same for all pixels, this change in normal direction implies a 0.1° change in the angle of reflection—which in turn implies the same change in the angle of incidence, for a combined 0.2° contribution to angular spread of incoming sunlight that gets reflected into the EPIC view direction. This implies that light from different parts of the 0.5° wide solar disk get reflected into the EPIC view direction from an approximately 25-km long area of the surface. Hence, regardless of scattering mechanisms at the surface, one expects EPIC to observe specular reflection in a region of at least 3–4 pixels depending on where pixel boundaries fall. Observations of glints over areas well beyond this size are then indicative of other causes such as scattering by rough surfaces or diffraction.

Because of the color filter wheel onboard, EPIC measurements at different wavelengths occur at slightly different times. This helps in identifying glints because the earth rotates by about 1° (∼100 km or ∼10 pixels) during the 4 min between the red and blue images, yielding slightly different viewing geometries for the two wavelengths and rendering the EPIC instrument multi-angular. This was exploited in [2] for automated detection of glints over land. The algorithm examined all locations with a small "*glint angle*" (the angle between EPIC view direction and the direction of specular reflection from a horizontal surface) and registered red or

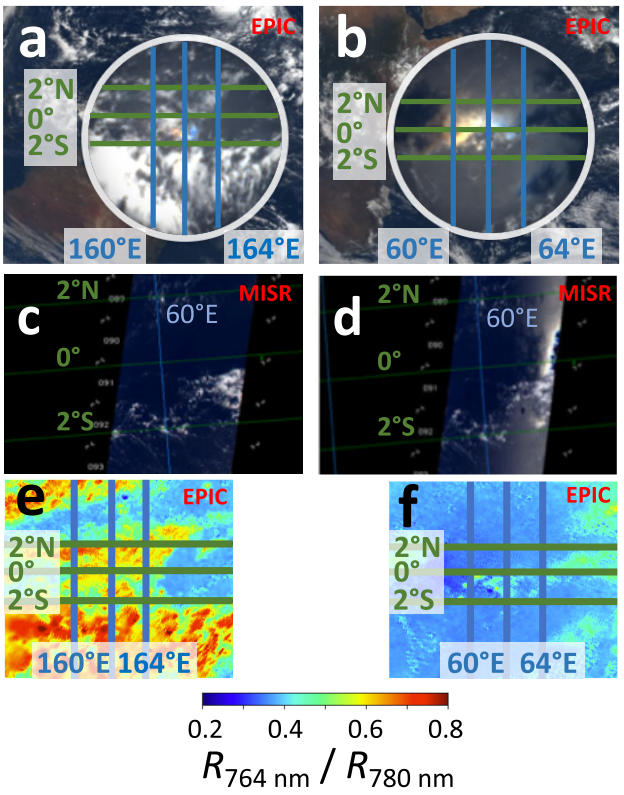

Fig. 1. Demonstration of EPIC's ability to distinguish ocean surface glints from clouds glints, and MISR's confirmation of this ability. (a) EPIC image of a glint from ice clouds over the ocean (Oct 3, 2015, 00:45 UTC). (b) EPIC image of a glint from the ocean surface (Oct 3, 2015, 07:27 UTC). These two images are from the EPIC website (epic.gsfc.nasa.gov). (c) and (d) West side of the glint in (b), as seen by two cameras of the MISR instrument: the oblique-looking Af camera and the nadir-looking An camera. Both panels are based on images obtained using the MISR online browse tool (https://l0dup05.larc.nasa.gov/MISR_BROWSE/). (c) Glint seen in (b) occurs in cloud-free regions. The glint appears only in (d) because of the difference in the view direction. The location of the glint shifts between (b) and (d) because of differences in the view direction of EPIC and MISR observations, and because the MISR image was taken an hour before the EPIC image. (e) and (f) Oxygen A-band (R_{764}/R_{780}) ratios for scenes in (a) and (b), respectively, with higher values indicating higher altitudes for (a) than (b), implying cloud and ocean glints.

blue glints when the ratio of 680- and 443-nm reflectances (R_{680}/R_{443}) exceeded the threshold value. The reflectance ratio thresholds were set so as to be exceeded much more often in potentially glint-containing parts of EPIC images than in nearby glint-free reference regions. In this letter, where all data are over the ocean, these nearby "glint-free reference regions" are selected to ensure they do not exhibit high reflectance ratios due to glints from the rough ocean surface.

To demonstrate (to the best of our knowledge for the first time) EPIC's ability to distinguish glints off clouds from glints off the ocean surface using oxygen A-band data, Fig. 1 shows two examples from oceanic regions observed on the same day. Fig. 1(a) shows a glint from ice crystals floating in clouds north of Australia, whereas Fig. 1(b) shows a glint from the surface of the Indian Ocean, just east of Somalia. The origin of glints in Fig. 1(a) and (b) can be confirmed by the A-band ratio (R_{764}/R_{780}), which can constrain altitude because oxygen absorbs sunlight at 764 nm, but not at 780 nm. Therefore, low (high) ratios indicate reflection from low (high) altitudes, as they imply that the signal passed through a thick (thin) atmospheric layer between the top of the atmosphere and the location of specular reflection. Fig. 1(e) and (f) shows A-band ratios around 0.6 (corresponding to cloud top height ~6.5 km in simulations) and 0.35 (corresponding to surface in clear areas) for the glints in Fig. 1(a) and (b), indicating cloud and surface glints, respectively. Toward a microphysical interpretation, we digress briefly to take a ~20 °C tropical ocean surface temperature, a 6 °C/km moist adiabatic lapse rate, and a 6.5 km cloud top height (resulting in 39 °C temperature drop), to arrive at a −19 °C cloud top temperature, practically ensuring plenty of ice crystals, irregularly shaped, and of various habits, including plates capable of particularly well-focused specular reflection when properly oriented [5], [6].

As further observational evidence of surface-cloud separation, Fig. 1(c) and (d) shows images by two cameras of the Multi-angle imaging spectro-radiometer (MISR) covering the left side of the area in Fig. 1(b). Panel (c) shows that the 26° tilt of the oblique-looking (Af) camera does not allow it to observe any glints, even though the nadir-viewing (An) camera shows a strong glint in cloud-free areas as shown in Fig. 1(d). Instead, Fig. 1(c) shows that the areas where Fig. 1(b) features a colorful glint (around and just north of the equator) are cloud free. Therefore, the MISR observations can be viewed as independent confirmation of EPIC's ability to separate ocean and cloud glints. We note that while the north-south extent of the glint in Fig. 1(b) is limited by low clouds, the east-west extent of the glint in the middle section of Fig. 1(d) is probably limited by changes in surface roughness caused by either winds or ocean currents.

While in Fig. 1, we chose individual scenes to illustrate EPIC's separation of ice cloud and ocean surface glints, in Fig. 2(a) we examine the results of such separation statistically for a yearlong data set of all EPIC images collected between November 1, 2016 and October 31, 2017. The histogram of A-band ratios features a bimodal distribution, and it is tempting to interpret the two parts as two distinct populations that correspond to glints from the ocean surface and from ice clouds. Glints in the region between the two peaks are unlikely to originate from low-level clouds, which are warm in the tropical band of EPIC glints [2]. Rather, we think that these glints come partly from cloudy pixels or semitransparent clouds (e.g., thin cirrus from anvil outflows) that barely filter the underlying ocean glint and add only a weak cloud signal. Fig. 2(a) shows that ~60% of glints have A-band ratios less than 0.45 [abscissa of the local minimum, a reasonable separation threshold based on Fig. 2(a)]. With such a threshold, Fig. 2(a) implies that cloud glints are detected at a rate comparable to surface glints.

The brightness probability distribution function (PDF) of the detected glints in Fig. 2(b) shows that cloud glints are often brighter than surface glints. In addition to implications in atmospheric science, this finding can be of interest to astronomers in their search for exoplanets: while, to the best of our knowledge, exoplanet research has focused on ocean glints [3], [4], this result shows cloud glints to be brighter in EPIC images of earth.

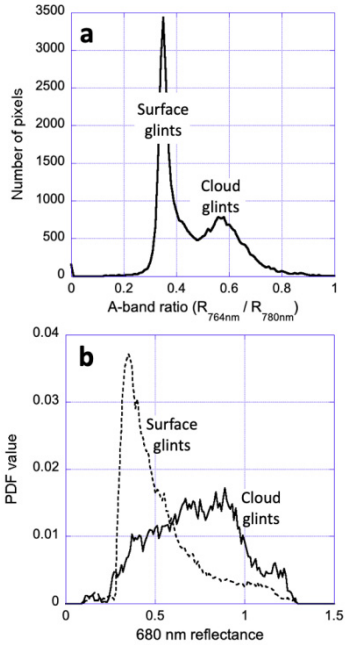

Fig. 2. Marine ice cloud glints appear ubiquitous and relatively bright: statistics of glint A-band ratios and reflectance values in a yearlong data set of EPIC images. (a) Histogram of the oxygen A-band ratio of red glints over the ocean. (b) PDF of red glint reflectance. The median 680-nm (red channel) reflectance for cloud and surface glints is 0.82 and 0.54, while the mode values are 0.89 and 0.35, respectively. Both panels consider all oceanic locations with glint angles $<1.5°$.

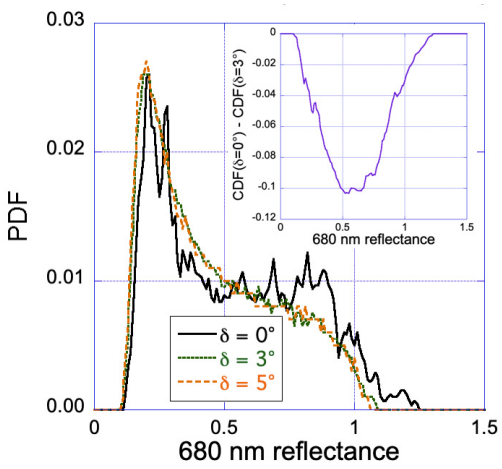

Fig. 3. Prevalence and angular extent of glints, based on reflectance variation: change in PDF of cloud reflectance values for various glint angles (δ). The inset shows the difference between the cumulative distribution functions (CDFs) for $\delta = 0°$ and $\delta = 3°$ (CDFs of the black and green curves). The figure is for the same yearlong data set as Fig. 2. The curves for larger δ are smoother because pixels are more numerous when we consider wider circles around $\delta = 0°$.

Fig. 2 shows that many cold (ice-containing) clouds are able to produce glints. To the extent that most of the ice particles in clouds are irregularly shaped, this implies that many ice particles are capable of specular reflection as long as they are optically large and have a horizontally oriented surface. But why are the cloud glints brighter than ocean glints on average? One possibility is that the bright glints off high clouds (e.g., cirrus) originate from large, horizontally oriented ice crystals [7], [8], in contrast to the wavy ocean surface that contain fine capillary ripples as well as a variety of gravity and wind-driven waves and thereby supply a wider variety of tilted facets that spread singly scattered radiation over a wider range of angles. Much of one's intuition about sea glitter comes from observations at grazing angles such as sunsets (where the Fresnel equations predict large reflection coefficients despite the high transparency of water), and so for EPIC conditions, one may wonder whether all that glitters is a glint. Still, the interpretation in terms of tilted facets on the ocean surface has a long and successful history at high sun elevations as well [9], and this interpretation is buttressed by the EPIC observations (see Fig. 1) that the spatial extent of ocean glints tends to be larger than that of cloud glints.

III. Size and Reflectance Distribution of Glints

While the previous section examined statistics of detected glints, this section examines the statistical impact of glints without identifying individual glints by the color ratio algorithm. Rather, we simply inspect the vicinity of all specular locations (where EPIC has small glint angles) over oceanic areas. We then examine reflectance values as a function of glint angle. This approach bypasses the uncertainties and somewhat arbitrary thresholds associated with the color ratio method of glint detection [2]. Moreover, by considering all data, we include even thin clouds and partly cloudy areas.

We now return to the question of the angular size of a typical specular spot (glint) in EPIC observations. How much brighter are the typical glints than their surroundings? To answer these questions, Fig. 3 presents three PDFs of 680-nm reflectance for all pixels identified as cloudy by the oxygen A-band ratio. The figure shows that the PDFs for 3° and 5° glint angles (δ) are nearly identical, which implies "blending" into background reflectance at these angular deviation values. We thus conclude that sun glints off marine clouds are confined to $\delta < 3°$ [Fig. 4(b) below suggests $\delta < 2°$]. As noted earlier, the $\sim$0.5° angular size of the solar disk and small uncertainties in pixel locations causes glints to spread over 3–4 pixels. Any spread beyond this can be attributed to the spread of tilt angles in nearly horizontally oriented ice facets, and to diffraction.

Fig. 3 also shows that the PDF of reflectance shifts toward higher values if the glint angle is small: the black curve is below (above) the green curve when $R_{680} < 0.55 (R_{680} > 0.55)$, which indicates that fewer (more) pixels have low (high) reflectance for $\delta = 0°$ than for $\delta = 3°$. The inset quantifies it: the difference between cumulative distributions for $\delta = 0°$ and for $\delta = 3°$ peaks around -0.1, indicating that the fraction of pixels with low (high) reflectance is about 0.1 less (more) for $\delta = 0°$ than for $\delta = 3°$. This suggests that for $\delta = 0°$, specular reflection from horizontally oriented particles (HOPs) increases the reflectance from below 0.55 to above 0.55 in about 10% of cloudy pixels. (The exact numbers vary somewhat with the definition of "cloudy.") We note, however, that 10% is a lower bound to the number of cloudy pixels affected by glints from HOPs; Fig. 2(b) shows that some glints are not bright enough to raise the reflectance above 0.55—and it is also likely that glints brighten some pixels whose reflectance would be above 0.55 even without glint. To put the 10%

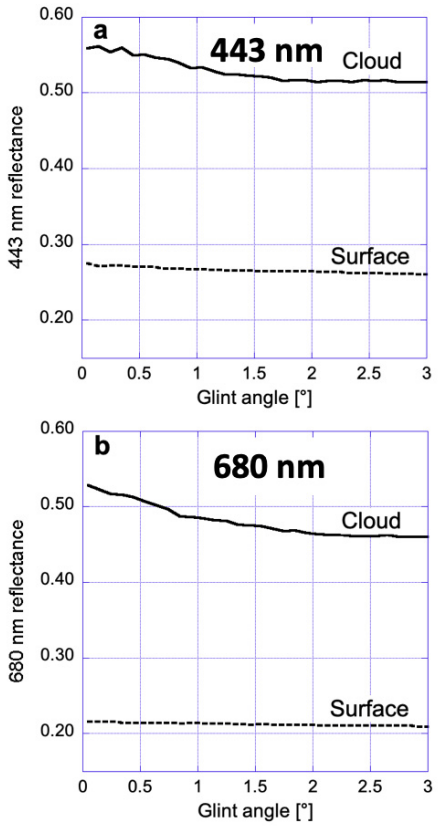

Fig. 4. Angular distribution of reflectance: reflectance values versus glint angle (δ). Reflectance increases around $\delta = 0°$ due to specular reflection from clouds and the ocean surface in both blue and red channels. (a) 443 nm. (b) 680 nm. It is seen that clouds and cloud glints reflect more intensely than ocean glints, consistent with Fig. 2(b). Note that since the data for this figure is not limited to glints (dominated by single scattering), the curve labeled "surface" includes the effect of multiple scattering in low clouds. The figure is for the same yearlong data set as Fig. 2.

lower bound in context, we examined the amount of liquid and ice clouds in the monthly average (Level-3) Moderate resolution imaging spectroradiometer (MODIS) cloud product (MOD06) [10], [11]. When averaged over the full year, the results indicated the ice phase for about 43% of clouds at the tropical marine regions where EPIC images have small glint angles in a given month. At this stage, however, we prefer to confine ourselves to parsimonious explanations guided by the actual observations and consider interpretation based on cloud microphysics as a conjecture. This is because a given reflectance value can be caused by many small HOPs within a pixel as well as by a few large ones, and exploring the possibilities for the disentanglement of size, concentration, and orientation effects will require significant further efforts.

We now return to our main theme of ocean versus marine ice cloud separation and use Fig. 4 to illustrate the impact of glints on overall reflectance. The hump of solid lines (marine ice clouds) at small glint angles shows that specular reflection from, say, oriented ice crystals, increases mean cloud reflectance by about 0.04 (8%) and 0.07 (14%) at 443 and 680 nm, respectively. The increase is smaller at the blue wavelength, possibly because of stronger Rayleigh scattering by the air above. The gentle shallow slope of the dashed curves is consistent with the hypothesis that specular reflection from the wavy and finely rippled ocean surface causes specular reflectance to spread over a wider range of viewing directions. In addition, capillary waves small enough to cause diffraction spreading may also contribute to the widening. We note that although the wider glints from ocean surfaces are often less bright than cloud glints, they can still be bright enough to foil measurements of water and atmospheric properties for a wide range of glint angles. For example, in an abundance of caution, the MODIS Dark Target aerosol retrievals exclude all data with $\delta < 40°$ [12].

Fig. 4 shows that the assumption of perfectly randomly oriented ice crystals might not be adequate, and radiative transfer simulations need to consider the scattering phase functions of HOPs [13]. We anticipate that combining such radiative transfer simulations with the kind of observations presented here will help researchers who have been interested in HOPs because of: 1) the spectacular optical phenomena they cause, such as subsuns, sun dogs, or circum-horizontal arcs [14], [15]; 2) their impact on the reflectivity of ice clouds [16]; and 3) the constraints their presence puts on humidity and temperature within clouds [5], [17]. In the past, simulations and ground-based, airborne, and satellite observations have yielded numerous insights about ice clouds and crystal orientation [6], [8], [18]–[22], but fundamental questions such as the frequency of HOPs persist [23].

Future glint studies are expected to help in addressing some of the remaining questions. First, the magnitude of the reflectance increase at small glint angles may help constrain the prevalence of HOPs (beyond the 10% lower limit). Also, the size and tilt distribution of HOPs may be estimated from the angular width of enhancements at red and blue wavelengths, which is determined mainly by two factors: 1) wavelength-dependent diffraction effects that are proportional to the ratio of wavelength and crystal size [24] and 2) wavelength-independent tilt of HOPs which, according to simulations, is $\sim 1°$, but is likely to increase with in-cloud turbulence and the Reynolds number, which in turn depends on crystal size [7], [8], [18]. We note that the slightly narrower cloud hump of the blue channel (vs. the red channel) in Fig. 4 is consistent with the diffraction spreading argument.

IV. Conclusion

The results, reported here, show that EPIC A-band data can distinguish glints off marine ice clouds from those off the ocean surface. Using this separation, it has been shown here that glints detected a million miles away from the earth often originate from marine ice clouds and that, indeed, such glints are ubiquitous. This opens the door to monitor and study cold marine clouds from deep space.

It has also been shown that glints off clouds are generally brighter but smaller in spatial extent than their ocean cousins. This surprising brightness of distant cloud glints raises the possibility of using glints in characterizing exoplanets without necessarily relying on liquid surfaces. It has also been demonstrated that glints off ice clouds have a discernible effect on the regional mean reflectance and EPIC observations can help constrain the radiative contribution of oriented ice crystals.

Earlier studies suggested that radiative properties of randomly and horizontally oriented (but otherwise identical) ice crystal populations [16] can differ substantially. To the extent that singly scattered light contributes to such radiative properties, future radiative transfer simulations, suitably constrained by the observed glint statistics described here, could estimate HOP contribution to cloud reflectivity, thereby improving our estimates of a key, yet highly uncertain aspect of climate: the impact of ice clouds on the solar heating of our planet [25], [26].

One can appreciate the possible range of the radiative impact of HOP glints vis-à-vis the commonly assumed random orientation from simple albeit approximate geometric considerations. In the Mie regime, relevant to visible observations of ice crystals, the scattering cross section of ice crystals can be approximated as twice the geometric one. Consider thin rectangular plates. For perfectly randomly orientations, one can use the Cauchy theorem to deduce that the total cross section is 1/4 of the particle surface area [27]. In contrast, HOPs fall so as to present the geometric cross sections equal to areas of largest resistance [7], [8] and so, for high sun, the geometric cross section is 1/2 of the total particle surface area. Thus, glinting oriented plates intercept roughly twice as much sunlight as the randomly oriented ones.

During the review process, we became aware of a recent publication by Li *et al.* [28] on a similar topic. While our work was done at about the same time, and results were obtained entirely independently by different means (e.g., relying on oxygen absorption) with a different focus (e.g., examining the impact of the glint on reflectances), we note now that our overall findings are consistent with [28].

Acknowledgment

The authors would like to thank P. Yang and C. Wang for insightful discussions on ice crystals and their radiative properties. They would also like to thank Y. Yang for sharing A-band simulation results. The EPIC and MODIS data were obtained from NASA LARC and GSFC data centers (https://eosweb.larc.nasa.gov/project/dscovr/dscovr_table and https://ladsweb.modaps.eosdis.nasa.gov), respectively.

References

[1] A. Marshak *et al.*, "Earth observations from DSCOVR EPIC instrument," *Bull. Amer. Meteorolo. Soc.*, vol. 99, no. 9, pp. 1829–1850, 2018. doi: 10.1175/BAMS-D-17-0223.1.

[2] A. Marshak, T. Várnai, and A. Kostinski, "Terrestrial glint seen from deep space: Oriented ice crystals detected from the Lagrangian point," *Geophys. Res. Lett.*, vol. 44, no. 10, pp. 5197–5202, May 2017. doi: 10.1002/2017GL073248.

[3] C. Sagan, W. R. Thompson, R. Carlson, D. Gurnett, and C. Hord, "A search for life on Earth from the Galileo spacecraft," *Nature*, vol. 365, pp. 715–721, Oct. 1993.

[4] J. Yaeger *et al.*, "Detecting ocean glint on exoplanets using multiphase mapping," *Astronomical J.*, vol. 156, no. 6, p. 301, 2018.

[5] M. P. Bailey and J. Hallett, "A comprehensive habit diagram for atmospheric ice crystals: Confirmation from the laboratory, AIRS II, and other field studies," *J. Atmos. Sci.*, vol. 66, no. 9, pp. 2888–2899, 2009. doi: 10.1175/2009JAS2883.1.

[6] V. Noel and H. Chepfer, "A global view of horizontally oriented crystals in ice clouds from Cloud-Aerosol Lidar and Infrared pathfinder satellite observation (CALIPSO)," *J. Geophys. Res.*, vol. 115, no. D4, Art. no. D00H23, 2010. doi: 10.1029/2009JD012365.

[7] J. I. Katz, "Subsuns and low Reynolds number flow," *J. Atmos. Sci.*, vol. 55, no. 22, pp. 3358–3362, 1998. doi: 10.1175/1520-0469(1998)055<3358:SALRNF>2.0.CO;2.

[8] F.-M. Bréon and B. Dubrulle, "Horizontally oriented plates in clouds," *J. Atmos. Sci.*, vol. 61, no. 23, pp. 2888–2898, 2004. doi: 10.1175/JAS-3309.1.

[9] C. Cox and W. Munk, "Measurement of the roughness of the sea surface from photographs of the sun's glitter," *J. Opt. Soc. Amer.*, vol. 44, no. 11, pp. 838–850, 1954. doi: 10.1364/JOSA.44.000838.

[10] S. Platnick *et al.*, "The MODIS cloud optical and microphysical products: Collection 6 updates and examples from Terra and Aqua," *IEEE Trans. Geosci. Remote Sens.*, vol. 55, no. 1, pp. 502–525, Jan. 2017. doi: 10.1109/TGRS.2016.2610522.

[11] S. Platnick *et al.*. (2018). *MODIS Cloud Optical Properties: User Guide for the Collection 6 Level-2 MOD06/MYD06 Product and Associated Level-3 Datasets*. [Online]. Available: https://modis-atmos.gsfc.nasa.gov/sites/default/files/ModAtmo/MODISCloudOpticalPropertyUserGuideFinal_v1.1_1.pdf

[12] L. A. Remer *et al.*, "The MODIS aerosol algorithm, products, and validation," *J. Atmos. Sci.*, vol. 62, no. 4, pp. 947–973, 2005. doi: 10.1175/JAS3385.1.

[13] G. Chen, P. Yang, G. W. Kattawar, and M. I. Mishchenko, "Scattering phase functions of horizontally oriented hexagonal ice crystals," *J. Quant. Spectrosc. Radiat. Transf.*, vol. 100, nos. 1–3, pp. 91–102, 2006. doi: 10.1016/j.jqsrt.2005.11.029.

[14] D. K. Lynch, "Atmospheric halos," *Sci. Amer.*, vol. 238, no. 4, pp. 144–153, 1978.

[15] G. P. Können, "Rainbows, halos, coronas and glories: Beautiful sources of information," *Bull. Amer. Meteorolo. Soc.*, vol. 98, no. 3, pp. 485–494, 2017. doi: 10.1175/BAMS-D-16-0014.1.

[16] Y. Takano and K.-N. Liou, "Solar radiative transfer in cirrus clouds. Part II: Theory and computation of multiple scattering in an anisotropic medium," *J. Atmos. Sci.*, vol. 46, no. 1, pp. 20–36, 1989.

[17] H. J. aufm Kampe, H. K. Weickmann, and J. J. Kelly, "The influence of temperature on the shape of ice crystals growing at water saturation," *J. Meteorol.*, vol. 8, no. 3, pp. 168–174, 1951. doi: 10.1175/1520-0469(1951)008<0168:TIOTOT>2.0.CO;2.

[18] D. K. Lynch, S. D. Gedzelman, and A. B. Fraser, "Subsuns, Bottlinger's rings, and elliptical halos ," *Appl. Opt.*, vol. 33, no. 21, pp. 4580–4589, 1994. doi: 10.1364/AO.33.004580.

[19] D. K. Lynch and W. Livingston, *Color and Light in Nature*. Cambridge, U.K.: Cambridge Univ. Press, 2001.

[20] K. Sassen and S. Benson, "A midlatitude cirrus cloud climatology from the Facility for Atmospheric Remote Sensing. Part II: Microphysical properties derived from lidar depolarization," *J. Atmos. Sci.*, vol. 58, no. 15, pp. 2103–2112, 2001. doi: 10.1175/1520-0469(2001)058<2103:AMCCCF>2.0.CO;2.

[21] H. Chepfer, G. Brogniez, P. Goloub, F. M. Bréon, and P. H. Flamant, "Observations of horizontally oriented ice crystals in cirrus clouds with POLDER-1/ADEOS-1," *J. Quant. Spectrosc. Radiat. Transf.*, vol. 63, nos, 2–6, pp. 521–543, 1999. doi: 10.1016/S0022-4073(99)00036-9.

[22] V. Noel and H. Chepfer, "Study of ice crystal orientation in cirrus clouds based on satellite polarized radiance measurements," *J. Atmos. Sci.*, vol. 61, no. 16, pp. 2073–2081, 2004. doi: 10.1175/1520-0469(2004)061<2073:SOICOI>2.0.CO;2.

[23] C. Zhou, P. Yang, A. E. Dessler, and F. Liang, "Statistical properties of horizontally oriented plates in optically thick clouds from satellite observations," *IEEE Geosci. Remote Sens. Lett.*, vol. 10, no. 5, pp. 986–990, Sep. 2013. doi: 10.1109/LGRS.2012.2227451.

[24] F. Crawford, *Waves, Berkeley Physics Course*, vol. 3. Berkeley, CA, USA: McGraw-Hill, 1968.

[25] J. R. Key, P. Yang, B. A. Baum, and S. L. Nasiri, "Parameterization of shortwave ice cloud optical properties for various particle habits," *J. Geophys. Res., Atmos.*, vol. 107, no. D13, p. 4181, 2002. doi: 10.1029/2001JD000742.

[26] N. G. Loeb *et al.*, "Impact of ice cloud microphysics on satellite cloud retrievals and broadband flux radiative transfer model calculations," *J. Climate*, vol. 31, no. 5, pp. 1851–1864, 2018. doi: 10.1175/JCLI-D-17-0426.1.

[27] A. B. Kostinski and A. Mongkolsittisilp, "Minimum principles in electromagnetic scattering by small aspherical particles," *J. Quant. Spectrosc. Radiat. Transf.*, vol. 131, pp. 194–201, Dec. 2013. doi: 10.1016/j.jqsrt.2013.08.006.

[28] J.-Z. Li *et al.*, "Study of terrestrial glints based on DSCOVR observations," *Earth Space Sci.*, vol. 6, no. 1, pp. 166–173, 2019. doi: 10.1029/2018EA000509.